Comparison of walleye pollock target strength estimates determined from *in situ* measurements and calculations based on swimbladder form

Kenneth G. Foote
Institute of Marine Research, 5024 Bergen, Norway

Jimmie J. Traynor
Northwest and Alaska Fisheries Center, National Marine Fisheries Service, National Oceanic and Atmospheric Administration, Seattle, Washington 98115

The target strength of walleye pollock (*Theragra chalcogramma*) at 38 kHz has been determined in each of two ways: (1) *in situ* measurement with dual-beam and split-beam echo sounders, and (2) theoretical calculation based on the swimbladder form. Respective probability density functions of target strength are compared. The several estimates of mean target strength ($\overline{TS}$) determine the relation $\overline{TS} = 20 \log l - 66.0$, where l is the fish fork length in centimeters.

PACS numbers: 43.20.Fn, 43.30.Gv, 43.30.Sf, 43.80.Jz

INTRODUCTION

The walleye pollock fishery is one of the world's largest.[1] The annual catch is about 6%–8% of the world's catch. Total estimated biomass on the eastern Bering Sea shelf and slope has ranged from 7 to 11 million tons in recent years.[2,3] Of this, over 50 percent is estimated to be in midwater.

A key ingredient in the conventional echo integration method of determining fish density absolutely is the fish backscattering cross section or target strength (TS).[4] An error in this quantity will have a first-order effect on the estimate of fish density.[5,6]

The target strength of walleye pollock has a significant history of measurement.[7,8] However, both the situation-dependent nature of the quantity[9] and recent developments in calibration, acoustic instrumentation, and theoretical modeling argue for a new examination.

In this study, the target strength of walleye pollock has been determined by (1) measurement with dual-beam and split-beam echo sounders,[10–13] and (2) calculation based on mappings of the swimbladder form.[14] The results are examined for both internal consistency and consistency with other determinations of gadoid target strengths. The possibility of using calculations in conjunction with direct *in situ* measurements to determine fish behavior is also considered.

I. MATERIALS AND METHODS

A. *In situ* measurements

The acoustic measurements and associated midwater trawl catch data of walleye pollock were obtained from a suitable aggregation of walleye pollock in the eastern Bering Sea (Fig. 1) on 1–2 August 1985. The procedures for data collection and analysis have been fully described by Traynor and Ehrenberg.[15] Some details are quoted here.

1. Acoustic system

The echo sounding system is a versatile system that provides appropriate signals for echo integration, as well as dual-beam and split-beam target strength analyses (Fig. 2). The transmitter uses a 5-kW pulse amplifier (Instruments, Inc. model SPG-4B). The receiving system is a prototype instrument constructed by Biosonics, Inc. The transducer (Fig. 3) was modified from a dual-beam transducer and is constructed using 79 individual ceramic elements, each approximately 13 mm in diameter. All elements are used during pulse transmission, while the elements are separated into five receiving segments. The center seven elements are separated to provide the signal for the wide beam of the dual-beam system. The remaining 72 elements are separated to form the four quadrants, consisting of 18 elements each, used to produce the split-beam signals. Five transmit/receive switches, housed in the transducer, are used to protect the receiving circuitry during pulse transmission. On reception, the signal from each transducer segment is amplified by a preamplifier in the transducer and relayed on separate conductors through the cable to the receiving hardware. Here, the segments are combined, prior to time-varied-gain (TVG) control, to form four half-beams for split-beam analysis and a sum beam. The sum-beam signal, used for both echo integration and target strength analyses, is provided to separate receiving circuits with appropriate TVG functions. System specifications are as follows: frequency, 38 kHz, nominal pulse duration, 0.6 ms, bandpass filter width to − 3-dB points, 4.5 kHz, narrow/wide beamwidths to − 3-dB points, 6/25 deg, and source level, 218 dB *re*: 1 μPa.

Dual-beam target strength measurement and echo integration measurements are completed using a Hewlett–Packard 1000-F computer. Single targets are accepted on the basis of half-amplitude pulse width in the narrow beam. The analysis procedures have been well described.[7,10,16]
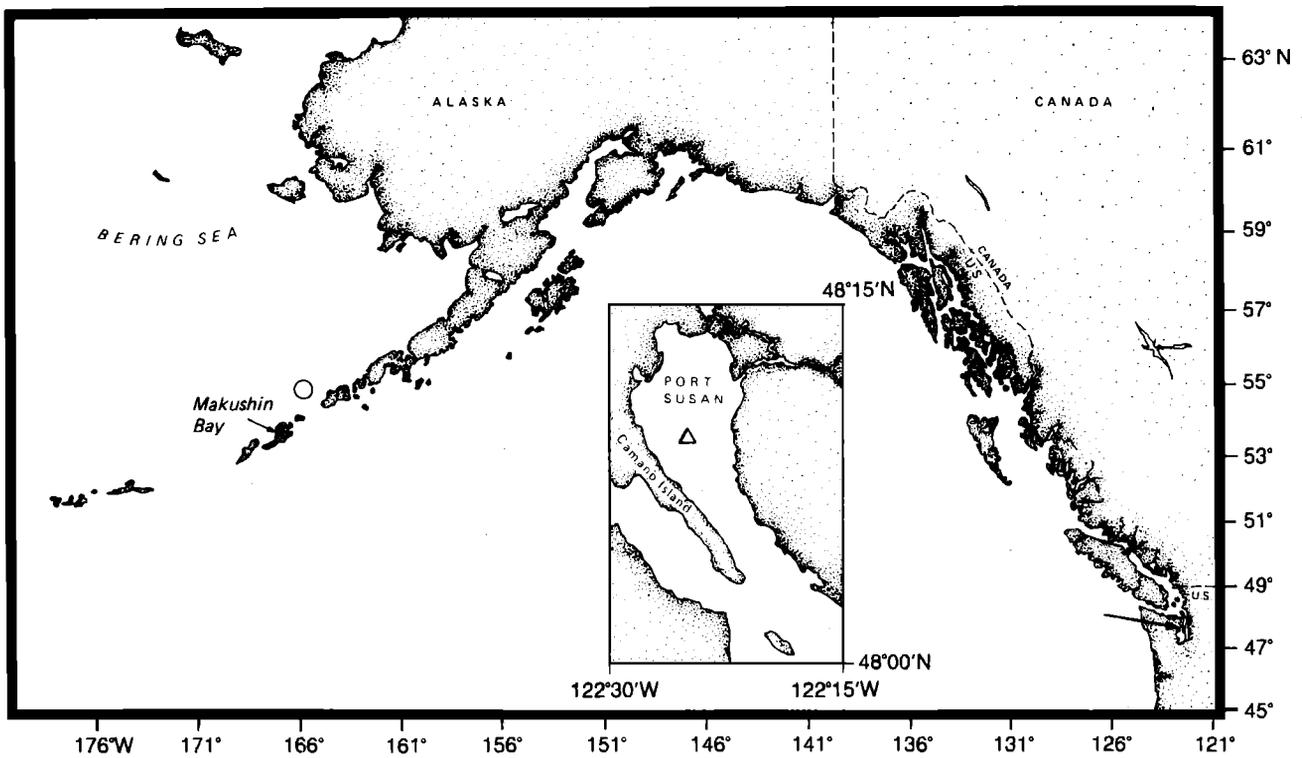
FIG. 1. Regions of data collection. Sampling sites: O = *in situ* target strength measurement; Δ = swimbladder morphology collection.

The split-beam phase measurement is accomplished using a prototype split-beam digital processor (SBDP) manufactured by Biosonics, Inc. The SBDP has been described by Hsieh.[17] The processor has, as hardware inputs, the synchronization pulse for the system and the outputs of the four half-beam receivers, namely, A + B, C + D, A + C, and B + D (Fig. 3), heterodyned to 10 kHz, and the detected sum

beam, all with 40 log r + 2ar TVG control. Operator inputs include sum-beam noise threshold, half-amplitude echo width acceptance window, and depth range to be analyzed.

2. Calibration of the acoustic system

Before and after each cruise, the system is calibrated using a standard technique to estimate the transmitting and
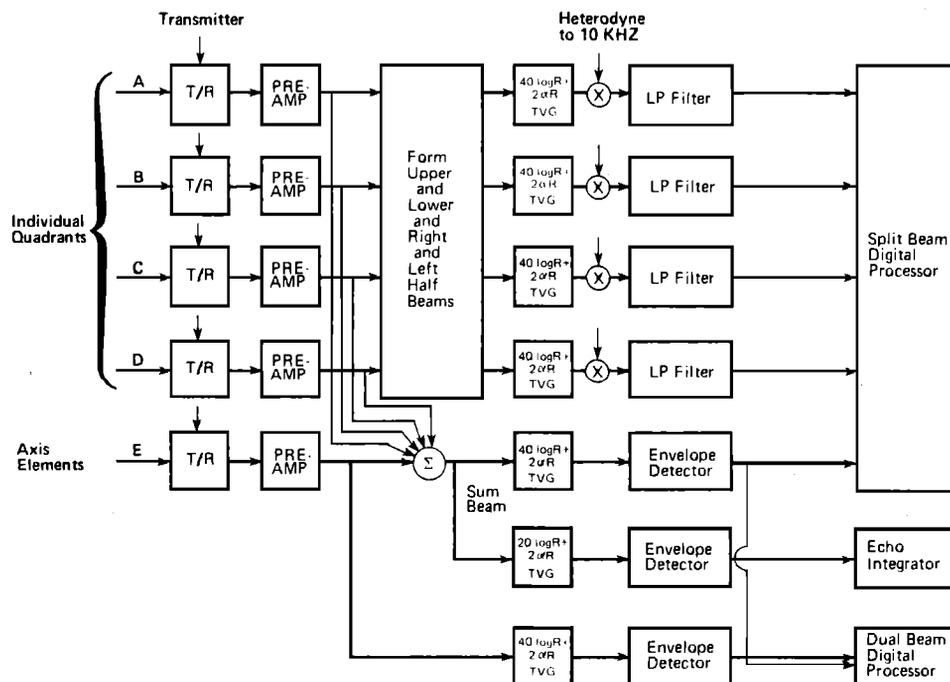
FIG. 2. Block diagram of echo sounding system, with signals for echo integration and dual-beam and split-beam target strength analysis.
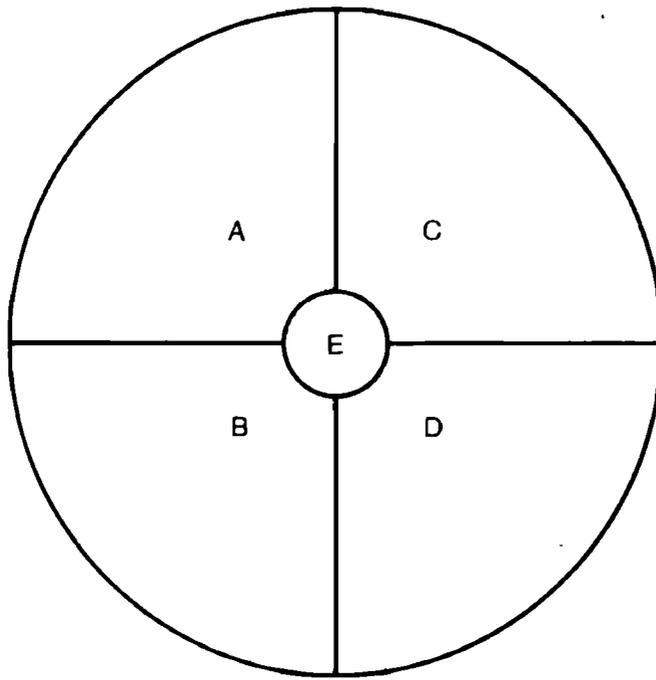
BEAM DESCRIPTION	TVG	USE	OUTPUT SIGNAL
A + C	40 log R + 2αR	Split-beam phase measurement	10 kHz
B + D	40 log R + 2αR	Split-beam phase measurement	10 kHz
A + B	40 log R + 2αR	Split-beam phase measurement	10 kHz
C + D	40 log R + 2αR	Split-beam phase measurement	10 kHz
E	40 log R + 2αR	Dual-beam, wide-beam amplitude	detected
A + B + C + D + E	40 log R + 2αR	Dual-beam, split-beam, narrow-beam amplitude	detected
A + B + C + D + E	20 log R + 2αR	Echo integration	detected

FIG. 3. Diagram of the dual-beam/split-beam transducer, showing the location of the various segments described in the text and the form of each beam used in the split-beam or dual-beam receivers.

receiving characteristics of the system. The amplitude characteristics of the receiver are monitored in the field using a calibration oscillator located in the transducer. They are set during the initial system calibration to be equivalent to a known intensity at the transducer face. The same oscillator is also used to monitor phase stability in the receiving circuitry and to correct for any constant phase offset between the split-beam half-beams.

A special calibration procedure is employed to map the beam pattern, a necessary procedure for split-beam echo sounders noted by MacLennan and Svellingen.[18] This is done by means of a calibration facility at the Applied Physics Laboratory, University of Washington, Seattle, Washington. The facility can provide signal pulses at a known delay and at known angles from the acoustic axis. In particular, a constant intensity pulse is provided to the split-beam transducer on a 15×15 grid from -3.5 to 3.5 deg in each of two orthogonal directions, with each point separated from the next by 0.5 deg. At each location, approximately 15 phase measurements are made and the voltage of the constant intensity pulse is measured. From the voltage measurement, the beam pattern is determined for each of the data points on the observation grid. The data are used to produce an empirical relationship between the two phase angles measured by the split-beam system and the one-way directivity effect, or beam pattern. In this way, the residual deviation has been kept under 0.02, or ± 0.17 dB, and the mean residual for all data points has been kept under 0.01, or ± 0.08 dB.

The overall system calibration is accomplished by means of a standard target.[19] This is described in the following section.

3. Data collection procedures

Initial tests of the echo sounding system were carried out from the chartered fishing vessel F/V MORNING STAR in July and August 1985 during a combined echo integration and midwater trawl survey of the eastern Bering Sea. On 24 July 1985, a calibration of the system was performed using a standard calibration sphere in Makushin Bay, on Unalaska Island, Alaska (Fig. 1), where the bottom depth was 50 m. The calibration procedure involved suspending a 38.1-mm-diam sphere of tungsten carbide with 6% cobalt binder[20] approximately 28.5 m below the transducer-bearing towed body, or fin. The fin was then lowered from 2 to 20 m in the water column to examine the effect of transducer depth on system performance. The total system response (source level plus system receiving response) was 1.9 dB higher at 20 m. Previous measurements of the transducer using an anechoic chamber indicated only minor changes in total system response (+ 0.1 dB) between 15 and 60 m. The measurements presented in this article, which were collected with the transducer located at 100 m, used the standard target calibration information obtained at 20 m. Target strength measurements of the standard sphere were made using both the dual-beam and split-beam procedures.

On 1 and 2 August 1985, target strength measurements and associated midwater-trawl data were collected in the eastern Bering Sea (Fig. 1). The acoustic targets were identified using a Diamond 1000 pelagic trawl. The vertical mouth opening of the trawl was 15 m, and it contained 40.6-cm (16-in.) stretch-measure mesh in the wings and mesh sizes ranging from 81.3 cm (32 in.) forward to 8.9 cm (3.5 in.) in the cod end. The cod end was equipped with a 3.2-cm (1.25-in.) mesh liner. The average headrope depth for both trawls was 119 m. The acoustic data were collected over the depth interval 112–150 m.

For all target strength analyses, namely, fish and standard target measurements, the single target acceptance criterion was half-amplitude echo width. Because of differences between the dual-beam and split-beam techniques in (1) the location of sampling points and sampling frequency, and (2) the manner of effecting the echo width measurement algorithm, some targets were accepted using one technique and rejected using the other. This was especially true for small echoes, the waveforms of which are most affected by noise. In addition, for both the dual-beam and split-beam processors, if analysis is not completed by the time the next sync pulse occurs, the new ping is ignored. For the comparisons presented in this article, only targets that were accepted by both systems were included for analysis. For both systems, the beam pattern threshold was set to − 3 dB and the noise threshold was set to twice the rms noise level. The echo width acceptance window was 0.4–0.8 ms.

B. Theoretical calculations

1. Collection of fish specimens

Walleye pollock were caught on hook and line at depths ranging from approximately 8 to 12 m from the deck of R/V MILLER FREEMAN, a 66-m stern trawler, anchored in Port Susan Bay, Washington (Fig. 1) on 9–10 August 1986. Samples were collected between approximately 0600 and 0900 h local daylight time on 9 August and between 0500 and 0700 on 10 August. The fish were immediately transferred live to a tank roughly $1 \times 2 \times 2$ m deep. They were acclimated for periods ranging from 36 h for the first captured specimens to 6 h for the last.

Each fish was immersed for several minutes in an alcohol bath maintained at a temperature between − 15° and − 30 °C and stored in a shipboard freezer at − 35 °C. Of the 59 walleye pollock captured, 31 specimens were sent to the Institute of Marine Research, Bergen, for anatomical measurement of the swimbladder.

2. Swimbladder morphometry

This method, which is due to Ona,[21,22] consists of the following steps: encasing the frozen fish in a block of carboxymethyl cellulose (CMC) solidified at a temperature of − 70 °C, systematic sectioning with a precision cryomicrotome, photographing representative cross sections of the exposed swimbladder, and digitization of the contour of the inner swimbladder wall. The surface between pairs of contours on successive parallel slices is triangulated by means of an automatic numerical algorithm.[14] Effects of misalignment of the fish in the CMC block are removed by the appropriate mathematical rotations.

Of the 31 specimens available at the outset, one was sacrificed in learning where to trim the fish prior to encasement. Fourteen of the remaining 30 specimens were found to have intact swimbladders, but 5 of these were greatly distended and showed signs of internal bleeding, and, hence, were rejected, leaving a final sample size of 9. Some gross dimensions of these are shown in Table I. With the exception of the neglected first specimen, the masses were measured just prior to the morphometry and, hence, are probably slightly less than at the time of catching owing to the drying effect of cold storage.

To further assess the quality of the data, the buoyancy was estimated in the usual fashion[23,24] through the ratio of the swimbladder volume in milliliters to the fish mass in grams. The values of 3%–6% were judged reasonable by Egil Ona, Institute of Marine Research, Bergen.

3. Target strength computation

This was performed according to the procedure in Ref. 14. The backscattering cross section σ was thus computed according to the finite-element realization of the formula

$$\sigma = 4\pi \left| \lambda^{-1} \oint_{S} \exp(2i\mathbf{k} \cdot \mathbf{r}) \mathcal{H}(\hat{k} \cdot \hat{n}) \hat{k} \cdot \hat{n} \, dS \right|^2, \quad (1)$$

where λ is the acoustic wavelength, $\mathbf{k}$ is the wave vector in the source or backscattering direction $\hat{k} = \mathbf{k}/k$, $\mathbf{r}$ is the position vector of the surface element with infinitesimal area dS,

TABLE I. Gross dimensions of the investigated walleye pollock specimens with usable swimbladders. The swimbladder data derive from the triangulations.

Fish No.	Length (cm)	Mass (g)	Swimbladder	
			Surface area (cm²)	Volume (cm³)
5	41	⋯	64.1	25.5
9	37	355	43.8	11.3
10	42	386	50.7	17.9
11	40	324	51.0	14.0
17	39	362	42.9	15.4
19	40	345	58.1	19.8
21	38	377	39.0	10.8
24	36	298	49.2	14.8
27	35	266	39.7	11.3

$\hat{n}$ is the unit normal to dS at $\mathbf{r}$, and $\mathscr{H}(x)$ is the Heaviside step function with values 1 for $x>0$, $\frac{1}{2}$ for $x=0$, and 0 for $x<0$. The integration is performed over the entire surface S of the swimbladder. Equation (1) corrects the misprint in Eq. (1) of Ref. 14.

The expression applies in the so-called high-frequency or Kirchhoff limit. Accordingly, the surface field is that of the incident field for positive $\hat{k}\cdot\hat{n}$ and vanishes identically for negative $\hat{k}\cdot\hat{n}$. Thus effects of diffraction on the surface field itself are ignored.

Equation (1) also applies in the single-frequency limit. This incurs only negligible error for typical echo sounder frequencies and pulse durations, as already demonstrated in Ref. 14.

The target strength (TS) is related to σ by the usual definition,[25]

$$\mathrm{TS} = 10 \log (\sigma/4\pi), \qquad (2)$$

although with the use of SI units.

The dependence of the target strength on tilt angle, or angle between the horizontal and imaginary line connecting the root of the tail with the tip of the upper jaw, has been calculated for each of the nine specimens. The range $[-45,45]$ deg has been exactly covered. The frequency was assumed to be 38 kHz and the medium sound speed, 1490 m/s.

II. RESULTS

Length–frequency distributions for the two trawl hauls are shown in Figs. 4 and 5. The fork length was measured. This is about 97.5% of the total length according to R. Baxter of the Northwest and Alaska Fisheries Center, Seattle.

Associated acoustic measurements with the dual-beam and split-beam systems are also presented in Figs. 4 and 5. Included with these are theoretical probability density functions (pdf's) of target strength.

The theoretical pdf's are computed on an expanded TS base formed by scaling the computed TS functions of tilt angle θ according to the transformation:

$$\mathrm{TS}_{l'} = \mathrm{TS}_{l} + 20 \log l'/l, \qquad (3a)$$

$$\theta_{l'} - \theta_{\mathrm{TS}_{\max}} = (\theta_{l} - \theta_{\mathrm{TS}_{\max}})l/l', \qquad (3b)$$
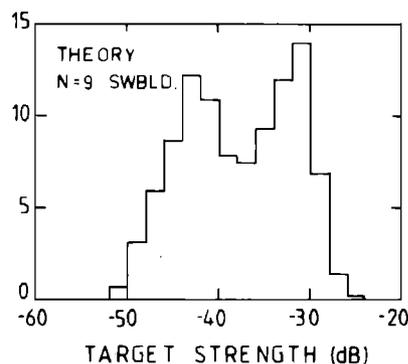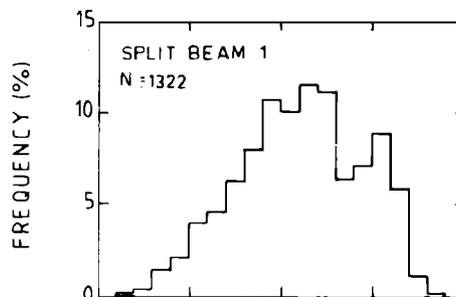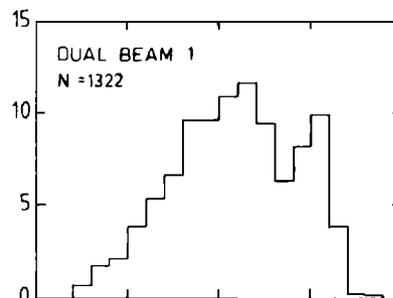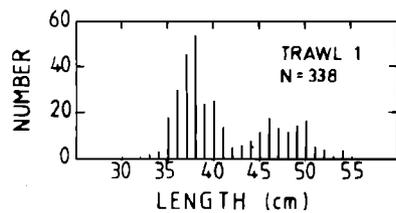
FIG. 4. Length–frequency distribution for trawl haul 1 and TS pdf's from dual-beam and split-beam measurements in sample 1 and from theoretical calculation based on nine swimbladders, the catch data for the trawl, and the tilt angle distribution $N(2,5)$.

where the subscripts l and l' denote fish lengths, and $\theta_{\mathrm{TS}_{\max}}$ denotes the tilt angle of maximum target strength value. Values lost by contracting the TS functions for $l' > l$ are supplemented with the constants $30 \log l - 100$. Each of the original nine TS functions is used to simulate a TS function at each centimeter interval of the range 30–55 cm, which spans those of the trawl catch data.

The pdf of each simulated function is computed separately with respect to the same pdf of tilt angle.[14] The individual pdf's are then averaged according to the weighting factors of the basis length–frequency distribution.

The described simulation has been repeated for a range of behavior modes for each of the two length–frequency distributions. The behavior modes are characterized by normal

FIG. 5. Length–frequency distribution for trawl haul 2 and TS pdf's from dual-beam and split-beam measurements in sample 2 and from theoretical calculation based on nine swimbladders, the catch data for the trawl, and the tilt angle distribution $N(2,5)$.

strength have been correlated. For the pdf's with values $\{f_i, i = 1,2,...,n\}$ and $\{g_i, i = 1,2,...,n\}$ over the TS domain from -60 to -20 dB in 2-dB steps, the correlation coefficient ρ is

$$\rho = \sum (f_i - \bar{f})(g_i - \bar{g}) \bigg/ \left(\sum (f_i - \bar{f})^2 \sum (g_i - \bar{g})^2 \right)^{1/2}, \tag{4}$$

where $\bar{f}, \bar{g}$ are the mean values, and the summations are performed over all n values.

The simulated pdf's with the highest correlation coefficients are shown in Figs. 4 and 5. The underlying tilt angle distribution is $N(2,5)$.

The pdf's with the largest correlation coefficients for each value of s_θ have also been identified in Table II. Included in this table are the corresponding averge backscattering cross section $\bar{\sigma}$ and so-called average or mean target strength $\overline{\text{TS}}$ formed by transforming $\bar{\sigma}$ in accordance with the standard definition in Eq. (2), viz.,

$$\overline{\text{TS}} = 10 \log (\bar{\sigma}/4\pi). \tag{5}$$

In averaging the measured data, the precise values, before reduction to histograms, were used. For convenience, the simulated histogram data were averaged by cell, where the mean backscattering cross section $\bar{\sigma}_{j,j+1}$ for cell j is

$$\bar{\sigma}_{j,j+1} = \frac{40\pi}{\ln 10} \frac{10^{\text{TS}_{j+1}/10} - 10^{\text{TS}_j/10}}{\text{TS}_{j+1} - \text{TS}_j}. \tag{6}$$

This is tantamount to assuming that the target strengths are uniformly distributed over the interval $[\text{TS}_j, \text{TS}_{j+1}]$. The width of the interval, $\text{TS}_{j+1} - \text{TS}_j$, is a constant 2 dB throughout the computations. Hence,

$$\text{TS} = m \log l + b \tag{7}$$

has been computed for $m = 20$ by substituting $\overline{\text{TS}}$ for TS and the mean length $\bar{l}$ for l. The result of determining b_{20} by regressing the individually averaged target strength functions of the original data base on corresponding lengths according to the same equation gives essentially identical results. The corresponding standard error of regression SE has been attached.

III. DISCUSSION

The measurements with the dual-beam and split-beam systems are very similar. This is evident from visual comparison of the measured histograms in each of Figs. 4 and 5. The respective correlation coefficients are 0.985 and 0.966. The mean target strengths, computed through the average backscattering cross section by Eq. (5), differ by 0.5 and 0.6 dB, with that due to the split-beam system being higher than the dual-beam number in both cases.

There is less similarity between the measured pdf's and the theoretical pdf's than between the two measured pdf's. Nonetheless, there is a distinct correspondence. This is witnessed by the correlation coefficients in Table II, which vary from 0.800 to 0.900. The theoretical averages are consistently lower than the measured averages, but not to any great extent. That is, the theoretical and measured averages are quite similar and may not be significantly different.

distributions of tilt angle, $N(\bar{\theta},s_\theta)$, and a uniform probability of occurrence in the circular region defined by the intersection of the horizontal plane with a right circular cone of 10-deg vertex angle. This was chosen somewhat arbitrarily for representing the likely maximum region of acceptance of single-fish echoes. In fact, the maximum angle of acceptance was consistent with a vertex angle of 6 deg. However, only negligible error was thus incurred.

Here, pdf's have been computed for each pair of values of $\bar{\theta}$ and s_θ from $\bar{\theta} \in \{-10, -9, -8,...,10\}$ deg and $s_\theta \in \{5, 10, 15\}$ deg. These have been supplemented by computations for $N(-4.4, 16.2)$, which is that observed by Olsen[26] for free-swimming spawning cod (*Gadus morhua*) in Lofoten.

Corresponding simulated and measured pdf's of target

TABLE II. Computational results based on length distributions of two trawl hauls and assumptions of normal distributions of tilt angle θ, including correlation coefficients of corresponding TS pdf's and averages of the observed dual-beam and split-beam data.

Data	$\bar{\theta}$ (deg)	s_θ (deg)	$\bar{\sigma}$ (cm²)	$\overline{TS}$ (dB)	b_{20} (dB)	SE (dB)	Pdf correlation coefficients Theory— dual beam	Theory— split beam
Trawl 1	2.0	5.0	45.5	−34.4	−66.7	1.5	0.900	0.872
Trawl 1	2.0	10.0	48.6	−34.1	−66.4	1.1	0.854	0.809
Trawl 1	−4.0	15.0	48.5	−34.1	−66.4	1.0	0.852	0.804
Trawl 1	−4.4	16.2	45.8	−34.4	−66.7	0.9	0.849	0.800
Dual-beam sample 1			48.9	−34.1	−66.4	0.2		
Split-beam sample 1			54.9	−33.6	−65.9	0.2		
Trawl 2	2.0	5.0	46.6	−34.3	−66.8	1.5	0.865	0.861
Trawl 2	1.0	10.0	53.5	−33.7	−66.2	1.1	0.840	0.840
Trawl 2	−4.0	15.0	50.1	−34.0	−66.5	1.0	0.840	0.828
Trawl 2	−4.4	16.2	47.3	−34.2	−66.8	0.9	0.836	0.820
Dual-beam sample 2			63.0	−33.0	−65.5	0.3		
Split-beam sample 2			72.3	−32.4	−64.9	0.3		

This observation is reinforced by the merest consideration of representativity. First, trawl haul 1 was performed at 1920 h local time on 1 August, while the acoustic data in sample 1 were collected at 0030 h on 2 August, that is, 5 h later. Also, trawl haul 2 was performed at 0240 h on 2 August, and the acoustic data in sample 2 were collected at 0400 h. Thus there may be a question as to whether the surveyed fish had the same length distribution as those present during the trawl. Second, if this were the case, the problem of trawl selectivity must still be addressed.[27–30] In the present case of the apparent length distribution of walleye pollock being 30–55 cm, the absence of effects in trawl selectivity would be remarkable.[31,32] Third, the representativity of the physical specimens collected for swimbladder morphometry of the surveyed fish may be questionable. To Ona,[22] the case for likely differences would be irrefutable. Given the general difficulty of raising caught walleye pollock to the surface without damaging the swimbladder, the authors have risked using specimens collected in Port Susan Bay, Washington, in August 1986 to represent fish surveyed in the eastern Bering Sea, 1000 miles away, in August 1985. The number of specimens (nine), moreover, is regrettably small.

That there is a measure of agreement between the theoretical and measured data does not surprise the authors. Detailed comparison of other in situ measurements and other theoretical simulations has been uniformly respectable.[33]

To illustrate, the intercepts b_{20} in Table II are compared through five examples. In each, the frequency is 38 kHz and the length measurement refers to total length. In the first three examples, involving measured or swimbladder-determined target strength functions of tilt angle, the averaging is performed with respect to Olsen's tilt angle distribution $N(-4.4, 16.2)$. (1) Based on averaging the TS functions of 171 gadoids spanning the lengths 6.7–96 cm, gathered by Nakken and Olsen in 1971,[34] $b_{20} = -66.3$, with SE = 1.5 dB. (2) Averaging of the TS functions of 86 pollack (Pollachius pollachius) spanning the lengths 26–44 cm, gathered by Foote in 1980,[35] determines $b_{20} = -67.3$, with SE = 1.0 dB. (3) Averaging the TS functions calculated on the basis of the triangulated swimbladder surfaces of 13 pollack and 2

saithe (Pollachius virens), gathered in 1980,[14,36] determines $b_{20} = -66.9$, with SE = 1.7 dB. (4) Combination of the mean in situ TSs of cod, saithe, and Norway pout (Trisopterus esmarki) with mean lengths of 14.8–81.6 cm, as measured with the SIMRAD split-beam echo sounder in 1984,[37] determines $b_{20} = -67.5$, with SE = 1.7 dB. (5) Simultaneous echo integration and counting of dispersed haddock (Melanogrammus aeglefinus) of mean length 43.8 cm, by Ona and Hansen in 1986,[38] determines $b_{20} = -67.7$, with a conservative confidence interval of ± 2 dB.

The present values for b_{20} for walleye pollock are mostly slightly higher, but then so are the earlier in situ measurements cited in the Introduction, namely, Refs. 7 and 8. The reference of the walleye pollock data to fork length rather than total length explains $-20 \log 0.975 = 0.2$ dB of this higher level. The historical data determine $b_{20} = -65.9$, with SE = 2.3 dB. This may be compared with the present value formed by equal weighting of empirical and theoretical data in Table II according to the following scheme: Each value of the first three tilt angle distributions for each trawl haul data set is weighted by the factor 2, the theoretical values for the tilt angle distribution $N(-4.4, 16.2)$ are ignored, and each empirical value for each sample is weighted by the factor 3. The result is $b_{20} = -66.0$, with SE = 0.6 dB.

A further, most interesting, comparison may be made with data recently presented by Miyanohana et al.[39] They measured the dorsal aspect target strength functions of seven tethered walleye pollock of lengths 34.2–45.4 cm for tilt angles from -50 to 50 deg at each of four frequencies, namely, 25, 50, 100, and 200 kHz. Miyanohana et al. then averaged the respective functions with respect to the tilt angle distribution $N(-5,15)$ and regressed the computed means as in Eq. (7), with $m = 20$, thereby determining the values $b_{20} = -65.1$ dB at 25 kHz and -67.0 dB at 50 kHz. Linear interpolation at 38 kHz gives $b_{20} = -66.1$ dB.

Another source of confidence for the new data and their analysis is the finding that the highest correlation coefficients were obtained for tilt angle distributions with means near the horizontal. The significance of this finding is under-

lined by the observed degree of upwards inclination of the swimbladder with respect to the axis or centerline of the fish. As measured by the negative of the angle of maximum target strength, denoted $\theta_{TS_{max}}$ earlier, this varied from 6.0 to 10.25 deg for the nine specimens.

For mean angles near ± 10 deg, differences between simulated and observed TS pdf's were large. Further, the kinds of tilt angle distributions associated with panic diving and fleeing reactions[40,41] are totally incompatible with the present acoustic measurements. Thus it may safely be assumed that the behavior of the surveyed walleye pollock was hardly, if at all, affected by the act of observation.

Were the data representativity assured, a refined determination of the underlying behavior pattern might be expected. As it is, the best agreement is obtained for the tilt angle distribution $N(2,5)$. Interestingly, this resembles the only tilt angle measurements on more or less free-swimming saithe,[42] a pelagivore like walleye pollock.[43]

It may also be noteworthy that the best agreement of measured and theoretical TS pdf's with $s_\theta = 15$ deg is obtained for $\bar\theta = -4$ deg. For the tilt angle distribution $N(-4,15)$, the correlation coefficients are only about 0.05 lower than the respective numbers for $N(2,5)$. But $N(-4,15)$ is essentially indistinguishable from $N(-4.4, 16.2)$, which is the only observed tilt angle distribution of free-swimming gadoids in the wild, namely, that of the benthopelagivore cod.[26]

IV. CONCLUSIONS

The present measurements and computations of walleye pollock target strength are basically consistent. Together they imply the following regression equation for use in acoustic determinations of fish density:

$$TS = 20 \log l - 66.0, \tag{8}$$

where l is the fish fork length in centimeters.

Differences are evident, however, between the measurements made with the dual-beam and split-beam systems and the computations based on swimbladder morphometries of nine specimens. Reasons for this may plausibly be sought in the representativity of the specimen swimbladders of those borne by fish plying the seas far away the previous summer.

Given conditions of representative sampling, as on a known aggregation with narrow length distribution, inference or deduction of fish behavior by comparing theoretical simulations with dual-beam or split-beam measurements may be expected. For the present subject aggregation, the tilt angle distribution is compatible with a normal distribution of near-horizontal mean and standard deviation of the order of 5–15 deg.

ACKNOWLEDGMENTS

[1]C. M. Lynde, M. v. Houten, and R. C. Francis, "Regional and temporal differences in growth of walleye pollock Theragra chalcogramma in the eastern Bering Sea and Aleutian Basin with implications for management," Contrib. "Workshop on comparative biology, assessment, and management of gadoids from the North Pacific and Atlantic Oceans," Seattle, Washington, 24–28 June 1985.

[2]J. J. Traynor and M. O. Nelson, "Overall results for pollock from the demersal and midwater surveys," Int. North Pac. Fish. Comm. Bull. 44, 216–222 (1985).

[3]J. J. Traynor, "Midwater abundance of walleye pollock in the eastern Bering Sea, 1979 and 1982," Int. North Pac. Fish. Comm. Bull. 45, 121–135 (1986).

[4]L. Midttun, "Fish and other organisms as acoustic targets," Rapp. P.-v. Reun. Cons. Int. Explor. Mer 184, 25–33 (1984).

[5]S. T. Forbes and O. Nakken, eds., "Manual of methods for fisheries resource survey and appraisal. Part 2. The use of acoustic instruments for fish detection and abundance estimation," FAO Man. Fish. Sci. 5, 1–138 (1972).

[6]K. A. Johannesson and R. B. Mitson, "Fisheries acoustics. A practical manual for aquatic biomass estimation," FAO Fish. Tech. Pap. 240, 1–249 (1983).

[7]J. J. Traynor and J. E. Ehrenberg, "Evaluation of the dual beam acoustic fish target strength measurement method," J. Fish. Res. Board Can. 36, 1065–1071 (1979).

[8]J. J. Traynor and N. J. Williamson, "Target strength measurements of walleye pollock (Theragra chalcogramma) and a simulation study of the dual beam method," FAO Fish. Rep. 300, 112–124 (1983).

[9]J. J. Traynor, "Dual beam measurement of fish target strength and results of an echo integration survey of the eastern Bering Sea walleye pollock (Theragra chalcogramma)," Ph.D. thesis, University of Washington (1984).

[10]J. E. Ehrenberg, "Two applications for a dual beam transducer in hydroacoustic fish assessment systems," Proc. IEEE Conf. Eng. Ocean Environ. 1, 152–155 (1974).

[11]J. E. Ehrenberg, "A comparative analysis of in situ methods for directly measuring the acoustic target strength of individual fish," IEEE J. Ocean Eng. OE-4(4), 141–152 (1979).

[12]J. E. Ehrenberg, "Analysis of split beam backscattering cross section estimation and single echo isolation techniques," Rep. Appl. Phys. Lab. Univ. Wash., No. APL-UW 8108 (1981).

[13]T. J. Carlson and D. R. Jackson, "Empirical evaluation of the feasibility of split beam methods for direct in situ target strength measurement of single fish," Rep. Appl. Phys. Lab. Univ. Wash., No. APL-UW 8006 (1980).

[14]K. G. Foote, "Rather-high-frequency sound scattering by swimbladdered fish," J. Acoust. Soc. Am. 78, 688–700 (1985).

[15]J. J. Traynor and J. E. Ehrenberg, "Fish and standard sphere target strength measurements obtained with a split beam–dual beam system," Contrib. "Symposium on fisheries acoustics," Seattle, Washington, 22–26 June 1987.

[16]J. J. Traynor and M. O. Nelson, "Calibration of a computerized echo integration and dual beam target strength measurement system," in Meet. "Hydroacoustical methods for the estimation of marine fish populations," Cambridge, Massachusetts, 25–29 June 1979, edited by J. B. Suomala, Jr. (Draper Laboratory, Cambridge, MA, 1981), Vol. 2, pp. 395–424.

[17]E. H. Hsieh, "Split beam target strength processor," M.S. thesis, University of Washington (1986).

[18]D. N. MacLennan and I. Svellingen, "Simple calibration technique for the split-beam echo-sounder," submitted to J. Acoust. Soc. Am.

[19]K. G. Foote, H. P. Knudsen, G. Vestnes, D. N. MacLennan, and J. Simmonds, "Calibration of acoustic instruments for fish density estimation: A practical guide," Coop. Res. Rep. Int. Counc. Explor. Sea 144, 1–69 (1987).

[20]K. G. Foote and D. N. MacLennan, "Comparison of copper and tungsten carbide calibration spheres," J. Acoust. Soc. Am. 75, 612–616 (1984).

[21]E. Ona, "Mapping the swimbladder's form and form-stability for theoretical calculations of acoustic reflection from fish," Cand. real. thesis, University of Bergen, Norway (1982) (in Norwegian).

[22]E. Ona, "Physiological factors causing natural variations in target strength," Contrib. "Symposium on fisheries acoustics," Seattle, Washington, 22–26 June 1987.

[23]A. D. Hawkins, "Fish sizing by means of swimbladder resonance," Rapp. P.-v. Reun. Cons. Int. Explor. Mer **170**, 122–129 (1977).

[24]F. R. Harden Jones and P. Scholes, "The swimbladder, vertical movements, and the target strength of fish," in Meet. "Hydroacoustical methods for the estimation of marine fish populations," Cambridge, Massachusetts, 25–29 June 1979, edited by J. B. Suomala, Jr. (Draper Laboratory, Cambridge, MA, 1981), Vol. 2, pp. 157–181.

[25]R. J. Urick. *Principles of Underwater Sound* (McGraw-Hill, New York, 1975), 2nd ed.

[26]K. Olsen, "Orientation measurements of cod in Lofoten obtained from underwater photographs and their relation to target strength," Counc. Meet. Int. Counc. Explor. Sea **1971/B**:17, Copenhagen, Denmark.

[27]B. B. Parrish, "A review of some experimental studies of fish reactions to stationary and moving objects of relevance to fish capture processes," FAO Fish. Rep. **62**, 233–245 (1969).

[28]G. Saetersdal, "Review of information on the behavior of gadoid fish," FAO Fish. Rep. **62**, 201–215 (1969).

[29]R. E. Craig, "Fisheries acoustics. Introduction," Rapp. P.-v. Reun. Cons. Int. Explor. Mer **184**, 5–6 (1984).

[30]C. S. Wardle, "Fish behavior and fishing gear," in *The Behavior of Teleost Fishes*, edited by T. J. Pitcher (Croom Helm, London, 1986), pp. 463–495.

[31]F. Cardador, "New experiments on trawl-mesh selection of hake on the Portuguese coast," Counc. Meet. Int. Counc. Explor. Sea **1986/B**:16, Copenhagen, Denmark.

[32]E. Ona and O. Chruickshank, "Haddock avoidance reactions during trawling," Counc. Meet. Int. Counc. Explor. Sea **1986/B**:36, Copenhagen, Denmark.

[33]K. G. Foote, "Fish target strengths for use in echo integrator surveys," J. Acoust. Soc. Am. **82**, 981–987 (1987).

[34]O. Nakken and K. Olsen, "Target strength measurements of fish," Rapp. P.-v. Reun. Cons. Int. Explor. Mer **170**, 52–69 (1977).

[35]K. G. Foote, "Linearity of fisheries acoustics, with addition theorems," J. Acoust. Soc. Am. **73**, 1932–1940 (1983).

[36]K. G. Foote and E. Ona, "Swimbladder cross sections and acoustic target strengths of 13 pollack and 2 saithe," Fiskeridir. Skr. Ser. Havunders. **18**, 1–57 (1985).

[37]K. G. Foote, A. Aglen, and O. Nakken, "Measurement of fish target strength with a split-beam echo sounder," J. Acoust. Soc. Am. **80**, 612–621 (1986).

[38]E. Ona and K. Hansen, "*In situ* target strength observations on haddock," Counc. Meet. Int. Counc. Explor. Sea **1986/B**:39, Copenhagen, Denmark.

[39]Y. Miyanohana, K. Ishii, and M. Furusawa, "Measurements and analyses on dorsal aspect target strength of six species of fish at four frequencies," Contrib. "Symposium on fisheries acoustics," Seattle, Washington, 22–26 June 1987.

[40]K. Olsen, J. Angell, F. Pettersen, and A. Løvik, "Observed fish reactions to a surveying vessel with special reference to herring, cod, capelin and polar cod," FAO Fish. Rep. **300**, 131–138 (1983).

[41]K. Olsen, "Fish behavior and acoustic sampling," Contrib. "Symposium on fisheries acoustics," Seattle, Washington, 22–26 June 1987.

[42]K. G. Foote and E. Ona, "Tilt angles of schooling penned saithe," J. Cons. Int. Explor. Mer **43**, 118–121 (1987).

[43]M. J. Allen, "Ecological segregation of fusiform gadoid fishes," Contrib. "Workshop on comparative biology, assessment, and management of gadoids from the North Pacific and Atlantic Oceans," Seattle, Washington, 24–28 June 1985.